## Journal of Materials Chemistry C



**View Article Online** 

### COMMUNICATION

Check for updates

Cite this: J. Mater. Chem. C, 2023, 11, 6290

Received 30th January 2023, Accepted 14th April 2023

DOI: 10.1039/d3tc00356f

rsc.li/materials-c

# Asymmetric diarylamine guests for a host-guest system with stimulus-responsive room temperature phosphorescence<sup>†</sup>

Jinzheng Chen,<sup>a</sup> Faxu Lin,<sup>a</sup> Guodong Liang, <sup>b</sup><sup>a</sup> Huahua Huang, <sup>b</sup>\*<sup>a</sup> Tian Qin,\*<sup>b</sup> Zhiyong Yang <sup>b</sup>\*<sup>bc</sup> and Zhenguo Chi <sup>b</sup>

The Förster resonance energy transfer (FRET) process has been utilized to construct host-guest systems with stimuli-responsive room-temperature phosphorescence (RTP). However, only two guests have been reported for these systems. Thus, the design of new guests and investigation of their molecular structural effects on their RTP properties has become an important and challenging work for improving their stimuli-responsive performance. In this work, a series of asymmetric diarylamine guests were designed and prepared for the DMAP host to construct host-quest systems, which exhibited stimuli-responsive RTP to heating, pressing, grinding and pH values; and it was revealed that the FRET process changes were the key to the stimulus-responsive RTP, by careful investigation. Interestingly, the host-guest system of DMAP/MDPA-Ph showed the best RTP performance, in which the T<sub>1h</sub> state of the host is close to the center between  $S_{1g}$  and  $T_{1g}$  states of the guest. Based on the time-resolved characteristics of RTP of these systems, anti-counterfeiting applications could be achieved through screenprinting or stamping processes. This work thus opened up a way to achieve excellent performance of stimulus-responsive RTP materials through molecular design of the guest.

#### Introduction

Metal-free organic room-temperature phosphorescence (RTP) has drawn tremendous attention due to its long-lived excited

state nature and its potential value in bioimaging,<sup>1</sup> data encryption,<sup>2</sup> organic light-emitting diodes (OLEDs),<sup>3</sup> optical storage,<sup>4</sup> and other applications.<sup>5,6</sup> So far, there are a lot of successful examples of stimulus-responsive RTP materials.<sup>7–9</sup> However, it is still challenging to construct efficient organic RTP systems, which are limited by the ineffective intersystem crossing (ISC) and the susceptible character of triplet excited states under ambient conditions. Therefore, many strategies have been proposed to improve the development of organic RTP materials, such as the heavy-atom effect,<sup>10</sup> H-aggregation,<sup>11</sup> hydrogen bonding, excitonic coupling<sup>12</sup> and hostguest systems.<sup>13-17</sup> Among them, host-guest systems are worthy of attention due to the hosts having special functional groups, such as carboxyl and carbonyl, which increase molecular interaction with the guests and promote the ISC in the guests for RTP, and can be regarded as ideal candidates to develop efficient organic RTP materials.<sup>18</sup>

Previous studies have shown that polymers such as poly(methyl methacrylate) (PMMA), polyvinyl alcohol (PVA), or supramolecules like cucurbit[7]uril (CB[7]) with a rigid environment can act as the matrix to encapsulate the guest emitters into it.19,20 The molecular interactions between the hosts and guests suppressed the nonradiative decay route, which is crucial in improving the quantum yields of RTP in these systems. Besides polymeric and supramolecular host matrixes, small molecular hosts are another promising candidate for activating efficient RTP emission.<sup>21,22</sup> The main advantage of the small molecular hosts is that they can be obtained from the commercial route or can easily modify their properties using molecular modification. Firstly, small molecular hosts can play roles in the oxygen barrier to avoid the sensitive excited triplet quenched by an air atmosphere and act as a "solution" to dilute guest emitter molecules to reduce the self-aggregation quenching effect, leading to restricting nonradiative decay to achieve RTP emission. Moreover, the small molecular hosts can involve their triplet states in the exciton transfer process of the singlet to the triplet states of the guest emitter by precisely

<sup>&</sup>lt;sup>a</sup> School of Materials Science and Engineering, Sun Yat-sen University,

Guangzhou 510275, P. R. China. E-mail: huanghh27@mail.sysu.edu.cn <sup>b</sup> Key Laboratory for Polymeric Composite and Functional Materials of Ministry of Education, Guangdong Engineering Technology Research Center for

High-performance Organic and Polymer Photoelectric Functional Films, School of Chemistry, Sun Yat-sen University, Guangzhou 510275, P. R. China. E-mail: qint7@mail.sysu.edu.cn

<sup>&</sup>lt;sup>c</sup> Guangdong Provincial Key Laboratory of Optical Chemicals, XinHuaYue Group, Maoming, 525000, P. R. China. E-mail: yangzhy29@mail.sysu.edu.cn

<sup>†</sup> Electronic supplementary information (ESI) available. See DOI: https://doi.org/ 10.1039/d3tc00356f

manipulating the energy levels, which can minimize the energy gap between the singlet and triplet energies ( $\Delta E_{\rm ST}$ ), thus enhancing the spin–orbit coupling to accelerate the ISC process to realize phosphorescence emission under ambient conditions.<sup>15</sup>

Förster resonance energy transfer (FRET) has improved the RTP system with NIR-persistent luminescence or stimulusresponsive properties.<sup>16</sup> The characteristics of FRET include close distance (<10 nm) between the host and guest as well as non-radiative transfer, which is a distance-sensitive energytransfer process mediated by a virtual photon.<sup>17</sup> In this system, the host DMAP with double nitrogen atoms could promote the formation of intermolecular hydrogen bonds to provide a rigid condition to suppress these non-radiative processes of the guest. On the other hand, the host's emission spectra overlapped the guest's absorbance, proving the FRET effect in this host-guest system. Recently, Li and Yang et al. reported another DMAP-based FRET host-guest doping stimulus-responsive RTP system,<sup>13,17</sup> obtaining tunable RTP colour by introducing the additional energy acceptor of fluorescein to construct ternary doping systems. However, only two guests have been used and investigated in these systems, which strongly limited the development of DMAP-based RTP systems with sensitive RTP properties. On the other hand, the detailed mechanism of these stimulus-responsive RTP systems also needed further study, which would provide clear guidance for designing novel hostguest RTP systems with multiple stimulus-responsive luminescence. In this work, a series of asymmetric diarylamine derivatives (MDPA-X) were chosen as guests, which were found to form stimulus-responsive RTP systems with the host DMAP based on the FRET process. Among these MDPA derivatives, the guest MDPA-Ph containing a biphenyl moiety showed enhanced higheffect RTP with a quantum yield of 15.8% and a lifetime of 0.78 s when doped into the DMAP host. After careful analysis, it was found that the suitable level of the triplet state of host DMAP between these singlet and triplet states of the guests can efficiently promote the ISC transition of the guests, resulting in an enhanced population of triplet excitons for RTP in these systems. Upon external stimuli, such as heat, pressure and grinding, the preliminarily mixed host and guest powder can realize RTP characteristics through the energy transfer process, which is related to decreasing the distance of host and guest molecules.

#### Results and discussion

In this work, the asymmetric diarylamine guest MDPA was purchased from a commercial route and recrystallized several times before being used. When we first conducted the research, the commercial MDPA acted as a guest doped into the DMAP host by a general procedure for preparing the host-guest doping system. The mixture of host and guest in suitable ratios (generally 1:100, molar ratio) was thoroughly dissolved into a solution and then the solvent evaporated to obtain the mixed product. However, the quantum yield and lifetime of RTP in this mixed sample were poor at 0.38% and 0.26 s, respectively. Journal of Materials Chemistry C

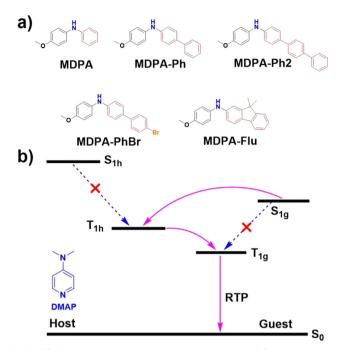


**Fig. 1** (a) Chemical structures of MDPA-X guests. (b) The proposed mechanism of exciton transition for promoting RTP inside these host–guest systems.

Thus, to enhance the RTP performance and carefully study the role of differences in the molecular structure on their RTP in the host–guest systems based on a DMAP host, a series of guests (MDPA-X), including MDPA-Ph, MDPA-Ph2, MDPA-PhBr, and MDPA-Flu (Fig. 1a) were synthesized *via* the Buchwald–Hartwig cross-coupling reaction. The detailed synthesis process and comparative spectroscopy data of their molecular structures are shown in the ESI† (Fig. S1–S3).

Surprisingly, MDPA-Ph, which combined the biphenyl moiety with the asymmetric diarylamine structure in the DMAP doping system (1:100, molar ratio), exhibited an attentiongrabbing RTP performance. The quantum yield and lifetime of RTP in this system were enhanced to be 15.8% and 0.78 s, respectively. Inspired by this, a series of asymmetric diarylamine derivatives based on MDPA-Ph have been designed and synthesized. The RTP properties of photos, spectra and intensity decay curves are shown in Fig. 2 and Fig. S4 (ESI<sup>+</sup>), respectively. Unfortunately, the quantum yield of the hostguest system of MDPA-Ph2 with an additional phenyl ring in its molecular structure dropped to 3.4%, despite its RTP lifetime still being long at 0.72 s. The heavy-atom effect was also considered and introduced into MDPA-Ph to improve the RTP efficiency of this host-guest system. Therefore the compound MDPA-PhBr containing a bromine atom was also designed and synthesized. Unfortunately, its RTP quantum yield and lifetime were less than those of MDPA-Ph, which were measured to be 10.8% and 0.66 s, respectively. The fluorene moiety is more rigid than the biphenyl group and widely utilized in building different advanced materials with special electronic or photonic properties,<sup>18–20</sup> inspiring us to replace the biphenyl group with the fluorene unit in MDPA-Ph. For the fluorene containing

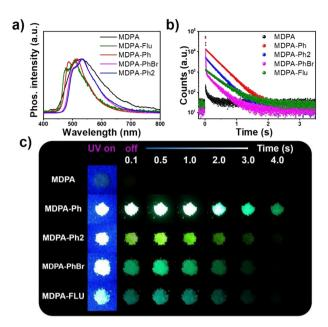


**Fig. 2** (a) The RTP spectra of DMAP doping systems with different guests. (b) Phosphorescence intensity decay curves of DMAP doping systems with different guests. (c) Photographs of DMAP doping systems with different guests, photographs were taken under a 365 nm UV lamp (on or off), and the times after the UV lamp was turned off are also given in the inset.

guest MDPA-Flu, the host–guest system showed an active RTP emission after the 365 nm UV light irradiation ceased. The emission could last approximately 10 s, resulting in a long RTP lifetime of 1.06 s. However, this system's quantum yield of 0.6% was the lowest among these systems. On comparison of the RTP spectra of these new guests, both MDPA-Ph2 and MDPA-PhBr exhibited similar RTP spectra to that of MDPA itself, while for the other two guests, the spectra of MDPA-Ph and MDPA-Flu possessed blue-shifted RTP peaks, as shown in Fig. 2a. Hence, the MDPA-Ph system exhibited the best RTP performance and was taken to explore further its stimulus-responsive properties and application in reversible pH-responsive sensors and anticounterfeiting ink.

Before investigating the stimulus-responsive RTP performance of the system, several photophysical properties of MDPA-Ph were studied. The DMAP molecules have been proven to form a rigid environment when they act as a host.<sup>17</sup> The phosphorescence of MDPA-Ph in solution at 77 K was checked and no RTP signal was observed in this solution (Fig. S4b, ESI<sup>†</sup>). This indicated that the ISC process in MDPA-Ph was poor and RTP could not be induced by simply putting it inside a rigid environment, such as doping into a rigid host. Then the energy levels of the host and guest in this system were calculated from their experimental data of cyclic voltammograms (Fig. S5a, ESI<sup>†</sup>) and the highest occupied molecular orbital (HOMO) and lowest unoccupied molecular orbital (LUMO) of the guest were found to be well sandwiched by those of the host DMAP (Fig. S5b, ESI<sup>†</sup>). In addition, a spectral overlap could be observed between the emission spectrum of the DMAP host and the absorption spectrum of the MDPA-Ph guest, as shown in

Fig. S6a (ESI<sup>†</sup>). Based on these results, the FRET process in the MDPA-Ph doping system (denoted as "MDPA-Ph@DMAP") could be inferred. Thus the DMAP molecule could play a role as an energy donor to transfer its energy to the acceptor MDPA-Ph, inducing the RTP in the doping system.

The effects of different MDPA-Ph guest ratios on the RTP properties of the MDPA-Ph@DMAP system, including phosphorescence spectra, decay curves and photographs were also investigated and are summarized in Fig. S8 (ESI<sup>+</sup>). It was revealed that the strongest RTP emission could be achieved in the doping systems with guest MDPA-Ph of a 1% molar ratio. According to Fig. S8 (ESI<sup>†</sup>), when the doping molar ratio of MDPA-Ph in the system was decreased to 0.1%, the resulting RTP intensity became very weak, indicating that the MDPA-Ph guest was diluted in the DMAP host matrix and the FRET process was also poor. However, when the doping molar ratio of MDPA-Ph in the host-guest systems was above 2% or even more, the RTP emission was also weakened, which indicated that the MDPA-Ph@DMAP system was susceptible to concentration quenching upon aggregation. Thus, in the following stimuli-responsive RTP investigation, host-guest systems with 1% molar ratio of MDPA-Ph were chosen as investigated samples.

To investigate the stimulus-responsive RTP feature of the MDPA-Ph@DMAP system, heating the host and the guestmixed sample was used to propel the guest molecule approach to the neighbouring area of the host ones so that they can accelerate the molecular motion. The powders of host and guest were mixed and then heated at different temperatures for 5 min and the RTP test was performed after the sample cooled to room temperature. As shown in Fig. 3a and d, almost no RTP emission could be detected after the mixed sample of host DMAP and guest MDPA-Ph was heated at 30 or 60 °C, respectively. As the heating temperature was increased, the PL intensity of the mixed DMAP and MDPA-Ph sample was decreased (Fig. 3b), while its RTP intensity was increased (Fig. 3a and d). This indicated that heating could facilitate the FRET process prominently and subsequently promote the RTP in this host-guest system. It is worth noting that the duration of afterglow can reach more than 4 s after heating at 120 °C for about 5 min, leading to a high quantum yield of 16.5% and a long lifetime of 0.75 s at the moment (Fig. 3c and Fig. S9, ESI<sup>†</sup>). When heated up to 120 °C, the doping sample was in a molten state, as the melting point of DMAP was 114 °C. After cooling down to room temperature, this doping system exhibited the best RTP performance among all heat-treated samples, which was due to the good dispersion of MDPA-Ph in the DMAP host during the melting process. These results confirmed the heat-responsive RTP of the MDPA-Ph@DMAP system.

In addition to heating, the mechanical-responsive RTP characteristics of the MDPA-Ph@DMAP system were also evaluated. Firstly, grinding was chosen for the experiments (Fig. 4a), which has been widely used in the research of mechanoluminescent materials. After the mixed sample of host DMAP and guest MDPA-Ph with a molar ratio of 100:1 was

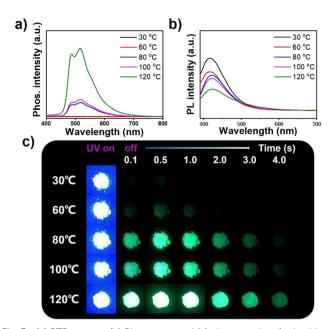
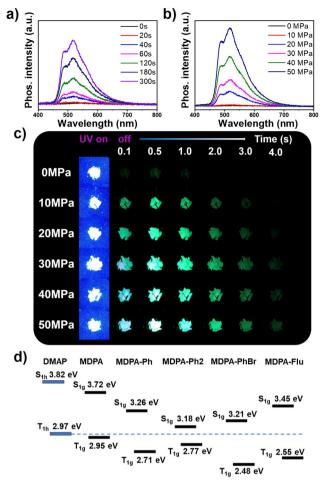


Fig. 3 (a) RTP spectra, (b) PL spectra, and (c) photographs of mixed host and guest (DMAP and MDPA-Ph with a molar ratio of 100 : 1) after heating at different temperatures (30–120 °C). Photographs were taken under a 365 nm UV lamp (on or off), and the times after the UV lamp was turned off are also given in the inset.

ground for about 20 s, the turn-on RTP emission could be detected. With the extension of the grinding time, the RTP intensity was further increased gradually, demonstrating a typical enhanced FRET process after grinding the mixed sample. Another mechanical measurement for the mixed sample was pressing, which was also widely used in the study of stimulus-responsive luminescence. As shown in Fig. 4b and c, the RTP was also enhanced obviously as the pressure increased from 10 to 50 MPa, which should be related to the sensitivity of FRET efficiency to the distance change between the host and guest molecules during pressure increase. Some reports suggested that it is due to the molecules' denser packing caused by high pressure that can strengthen the electronic interaction between the host and guest.<sup>17</sup> Compared with the powder X-ray diffraction (PXRD) patterns of the MDPA-Ph@DMAP samples after different treatments (Fig. S10, ESI<sup>+</sup>), similarly sharp and strong diffraction peaks were observed in these patterns. This means that these treated doping systems have a similar molecular packing and well-ordered crystalline state, which demonstrates that the enhanced RTP was not induced by different molecular packings after various treatments.

Related experiments and theoretical calculations were carried out to deeply understand the RTP process of the DMAP based host–guest doping systems. The absorption, emission, and excitation spectra of the host, guest and their mixture after heating at different temperatures have been measured (Fig. S6 and S7, ESI†). After separately heating the host and guest at different temperatures, very weak RTP for the DMAP host and no RTP for the MDPA-Ph guest were observed after the samples cooled down to room temperature (Fig. S7, ESI†). Regarding the



**Fig. 4** (a) RTP spectra of mixed host and guest (DMAP and MDPA-Ph with a molar ratio of 100:1) after grinding for different times. (b) RTP spectra and (c) photographs of mixed host and guest (DMAP and MDPA-Ph with a molar ratio of 100:1) under different pressures at room temperature. Photographs were taken under a 365 nm UV lamp (on or off), and the times after the UV lamp was turned off are also given in the inset. (d) The excited state arrangements of DMAP and guest molecules, determined by fluorescence and phosphorescence spectra.

absorption or excitation spectra, no changes could be found for the spectra of the MDPA-Ph guest (Fig. S6f and i, ESI†). A similar phenomenon for the DMAP host was observed below the heating temperature of 120 °C (Fig. S6e and h, ESI†). After heating at 120 °C, the emission of the host exhibited a bit of a redshift, while its excitation showed a bit of a blueshift. This is because of the melting and recrystallization process of the host during the heating (Fig. S6b, ESI<sup>†</sup>). Interestingly, there was a new peak appearing in the region from 325 to 450 nm in the absorption spectra of the mixture of MDPA-Ph@DMAP, with the increase in the heating temperature (Fig. S6g, ESI<sup>†</sup>). This should be due to the dispersing process of the guest into the host, which also induced broader and blueshift of the excitation spectra of the mixture of MDPA-Ph@DMAP as the heating temperature was increased. As a result, the emission of the guest could be easily excited beyond its excitation peak of about 375 nm for its solid, which was due to the FRET process from

the host DMAP to the guest. The excitation peak of the host was really in the blue region with a peak at about 320 nm (Fig. S6d, ESI<sup>+</sup>).

The energy arrangements of excited states and the possible transition channels for ISC transition of these guest molecules have been calculated from Gaussian. As shown in Fig. S11 (ESI<sup>+</sup>), only MDPA and MDPA-Ph2 exhibited one possible ISC transition channel from the computed results. However, these channels were either endergonic in MDPA or had a big energy gap in MDPA-Ph2, leading to inefficient ISC transitions. Therefore, all these MDPA guests showed no phosphorescence at room temperature. The values of the lowest singlet  $(S_1)$  and lowest triplet  $(T_1)$  states of the host DMAP and guest molecules were obtained according to their fluorescence and phosphorescence spectra. As shown in Fig. 4d, the T<sub>1h</sub> state of host DMAP was located between the  $S_{1\mathrm{g}}$  and  $T_{1\mathrm{g}}$  of these guest molecules, which can minimize the energy gap ( $\Delta E_{\rm ST}$ ) between the S<sub>1g</sub> and T<sub>1g</sub> of the guest through involving an intermediate stepping board to help excitons transfer from  $S_{1g}$  to  $T_{1g}$  of the guest, as explained for MDPA-Ph in Fig. 1b. Such minimized  $\Delta E_{\rm ST}$  could enhance the spin–orbit coupling to accelerate the ISC process, thus realizing RTP emission in these doping systems. Carefully analyzing the position of T<sub>1h</sub> of DMAP inset between the  $S_{1g}$  and  $T_{1g}$  of these MDPA derivatives, some interesting insights could be revealed. Firstly, the RTP performance improved in these host-guest doping systems when the position of  $T_{1h}$  was close to the center between  $S_{1g}$  and  $T_{1g}$ . For all these guests except MDPA, the T<sub>1h</sub> was located near the center, and thus they showed apparent RTP emission except for MDPA. Another conclusion is that the RTP intensity was decreased when the energy gap between  $T_{\rm 1h}$  and  $S_{\rm 1g}/T_{\rm 1g}$  exceeded 0.3 eV, for the case of MDPA-Flu. Regarding MDPA-Br, the energy gap of this system was also bigger than 0.3 eV. However, its RTP intensity was still good, which should benefit from the heavy atom effect of the bromide atom to enhance SOC coupling. Interestingly, for the guests MDPA, MDPA-Ph, and MDPA-Ph2, their  $S_{1g}$  and  $T_{1g}$ decreased significantly as the number of phenyl groups increased, indicating that it is an efficient way to modulate their excited state levels through controlling the number of phenyl groups and from the optimized electron cloud distributions of the HOMOs and LUMOs for DMAP and the guests in Fig. S12 (ESI<sup>†</sup>), it could be revealed that much more differences are shown in the distribution between the HOMO and LUMO in MDPA, MDPA-Ph2 and MDPA-PhBr, which would lead to the strong intramolecular charge transfer (ICT) state in their excited states. However, the distribution between the HOMO and LUMO was similar in MDPA-Ph and MDPA-Flu, resulting in the weak ICT state in their excited states. These results explained the blue-shifted RTP peaks of MDPA-Ph and MDPA-Flu (Fig. 2a).

The intermolecular interactions inside the doping system were also calculated, and the ground state geometries of MDPA-Ph doping mixtures with different ratios from 1:1 to 3:1 have been optimized and are shown in Fig. S13 and S14 (ESI<sup>†</sup>). As shown in Fig. S13 (ESI<sup>†</sup>), when the MDPA-Ph doping system is in a molecular dimer or trimer state with a ratio of 1:1 or 2:1, apparent intermolecular charge transfer (CT) from the occupied orbital of MDPA-Ph to the vacant orbital

of the host DMAP can be observed, which facilitates the ISC transition and the phosphorescence emission,<sup>13</sup> while the tetramer with DMAP: MDPA-Ph = 3:1 showed the  $\pi$ - $\pi$ \* transition from the HOMO of MDPA-Ph to its LUMO. Then, the corresponding SOC values between  $S_1$  and  $T_n$  of DMAP: MDPA-Ph = 1:1 and 2:1 were also calculated. It is believed that the range of energy level difference between  $S_1$  and  $T_n$  is less than 0.3 eV, plus larger SOC values of  $S_1$  to  $T_n$  facilitated the ISC process for RTP emission.<sup>18</sup> As shown in Fig. S14 (ESI<sup>†</sup>), due to intermolecular charge transfer, the largest SOC value of 0.2766 cm<sup>-1</sup> in DMAP: MDPA-Ph = 2:1 is S<sub>1</sub> to T<sub>4</sub> with an energy level difference of less than 0.3 eV. This was higher than that of 0.2445 cm<sup>-1</sup> in DMAP: MDPA-Ph = 1:1 (S<sub>1</sub> to T<sub>3</sub>), which is beneficial to enhance the RTP performance. These interactions between the host and guest thus facilitated the promotion of RTP in these doping systems.

Benefiting from the fact that the nitrogen atoms in the DMAP molecules can promote the formation of intermolecular hydrogen bonds,<sup>17</sup> the MDPA-Ph@DMAP system may be designed as a reversible pH-responsive sensor in an aqueous solution. As shown in Fig. S15 (ESI<sup>+</sup>), when the doping sample was treated with an acidic environment (pH = 5), the intensity of RTP emission was weakened (red dashed line). Then the sample was treated with a pH value of 9. It was found that the RTP intensity could be restored to half the intensity of the initial state (solid red line), not to the initial intensity. This might be due to the alkaline environment causing the breaking of the hydrogen bonding net, so the test sample cannot recover to its original state. After treating the sample with acid and alkaline solutions several times sequentially, the results showed good acid-base response repeatability with acid and base solutions of a range of pH values. It is noteworthy that there are few reports about small organic molecule based host-guest doping systems with RTP emission that can respond to various pH values in the aqueous environment.<sup>19,20</sup> An ink printing anti-counterfeiting application based on the MDPA-Ph@DMAP system has been made by a screen-printing method.

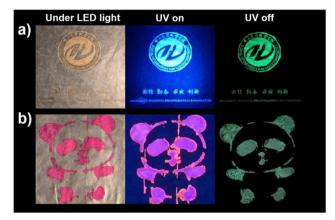


**Fig. 5** (a) Anti-counterfeiting application of the pattern of the department emblem and the motto. (b) Anti-counterfeiting application of the "panda" pattern with a third component rhodamine B doped (weighing paper as the substrate and realized by the screen-printing (a) and the stamping (b) process).

As shown in Fig. 5a, the pattern of the department emblem and the motto of "Solidarity, Diligence, Practicality and Innovation" could be written in Chinese and English displayed after the UV light irradiation ceased. Another ink with a third component of rhodamine B added into the MDPA-Ph@DMAP system has been prepared and used to stamp the panda pattern with a model. Under the UV light excitation, the "panda" pattern showed a pink colour. After turning off the excitation source, the "panda" pattern led to a celadon afterglow of green and pink colours, which were from MDPA-Ph and rhodamine B, respectively (Fig. 5b). These results indicated that this RTP system has great potential to be utilized in the anticounterfeiting field.

#### Conclusions

In summary, a series of new asymmetric diarylamine guests have been developed for the host-guest system based on a DMAP host, which exhibited prominent stimulus-responsive RTP characteristics. Through detailed research, it was found that the FRET process from host to guest was key to obtaining RTP emission in these host-guest doping systems. In addition, the best RTP performance could be achieved in the MDPA-Ph@DMAP system, when the T<sub>1h</sub> state is close to the center between the  $S_{1g}$  and  $T_{1g}$  states. Moreover, the effects on the FRET process of the external stimulus, such as heating, pressing and grinding, were carefully investigated, indicating that the FRET process changes were the key to the stimulusresponsive RTP. Based on plenty of intermolecular hydrogen bonds inside the doping system, a reversible pH-responsive sensor of MDPA-Ph@DMAP was prepared. The anticounterfeiting applications based on the time-resolved characteristics of RTP with these systems had been realized through screen-printing or stamping processes. This work has opened up a way to prepare organic stimulus-responsive RTP materials through molecular design of the guest. More work is being done in our laboratory to determine the detailed design principle of guests to achieve better performance in stimulusresponsive RTP systems.

#### Author contributions

Jinzheng Chen carried out the RTP experiments, Tian Qin conceived the molecular design idea and designed the synthetic experiments, and all the authors contributed to the data analysis. Tian Qin wrote the manuscript with the assistance of Zhiyong Yang, Huahua Huang and Zhenguo Chi. This work is supported by funds received by Tian Qin, Zhiyong Yang and Zhenguo Chi.

#### Conflicts of interest

There are no conflicts to declare.

#### Acknowledgements

This work was financially supported by the NSFC (51973239, 51873237, and 52073315), Guangdong Natural Science Funds for Distinguished Young Scholar (2017B030306012), Basic and Applied Basic Research Fund Project of Guangdong (2021A1515110119) and Fundamental Research Funds for the Central Universities.

#### Notes and references

- 1 Y. Wang, H. Gao, J. Yang, M. Fang, D. Ding, B. Z. Tang and Z. Li, *Adv. Mater.*, 2021, **33**, 2007811.
- 2 C. Qian, Z. Ma, X. Fu, X. Zhang, Z. Li, H. Jin, M. Chen, H. Jiang, X. Jia and Z. Ma, *Adv. Mater.*, 2022, 2200544.
- 3 J. Wang, B. Liang, J. Wei, Z. Li, Y. Xu, T. Yang, C. Li and Y. Wang, *Angew. Chem.*, *Int. Ed.*, 2021, **133**, 15463–15467.
- 4 Y. Wang, J. Yang, M. Fang, Y. Gong, J. Ren, L. Tu, B. Z. Tang and Z. Li, *Adv. Funct. Mater.*, 2021, **31**, 2101719.
- 5 M. Gmelch, T. Achenbach, A. Tomkeviciene and S. Reineke, *Adv. Sci.*, 2021, **8**, 2102104.
- 6 X. Wang, H. Shi, H. Ma, W. Ye, L. Song, J. Zan, X. Yao, X. Ou, G. Yang, Z. Zhao, M. Singh, C. Lin, H. Wang, W. Jia, Q. Wang, J. Zhi, C. Dong, X. Jiang, Y. Tang, X. Xie, M. Y. Yang, J. Wang, Q. Chen, Y. Wang, H. Yang, G. Zhang, Z. An, X. Liu and W. Huang, *Nat. Photonics*, 2021, **15**, 187–192.
- 7 W. Shao and J. Kim, Acc. Chem. Res., 2022, 55, 1573-1585.
- 8 H. Nie, Z. Wei, X.-L. Ni and Y. Liu, *Chem. Rev.*, 2022, **122**, 9032–9077.
- 9 H. Gao and X. Ma, Aggregate, 2021, 2, e38.
- 10 J. Wang, X. Gu, H. Ma, Q. Peng, X. Huang, X. Zheng, S. H. Sung, G. Shan, J. W. Lam, Z. Shuai and B. Tang, *Nat. Commun.*, 2018, 9, 1–9.
- Z. An, C. Zheng, Y. Tao, R. Chen, H. Shi, T. Chen, Z. Wang, H. Li, R. Deng, X. Liu and W. Huang, *Nat. Mater.*, 2015, 14, 685–690.
- 12 Z. Yang, Z. Mao, X. Zhang, D. Ou, Y. Mu, Y. Zhang, C. Zhao, S. Liu, Z. Chi, J. Xu, Y.-C. Wu, P.-Y. Lu, A. Lien and M. R. Bryce, *Angew. Chem.*, *Int. Ed.*, 2016, **128**, 2221–2225.
- 13 Y. Wang, J. Yang, Y. Gong, M. Fang, Z. Li and B. Z. Tang, *SmartMat*, 2020, **1**, e1006.
- 14 T. Wang, J. De, S. Wu, A. K. Gupta and E. Zysman-Colman, *Angew. Chem., Int. Ed.*, 2022, e202206681.
- 15 G. Qu, Y. Zhang and X. Ma, *Chin. Chem. Lett.*, 2019, **30**, 1809–1814.
- 16 L. Ma and X. Ma, Sci. China: Chem., 2023, 304-314.
- 17 X. Yan, H. Peng, Y. Xiang, J. Wang, L. Yu, Y. Tao, H. Li, W. Huang and R. Chen, *Small*, 2022, 18, 2104073.
- 18 S. Guo, W. Dai, X. Chen, Y. Lei, J. Shi, B. Tong, Z. Cai and Y. Dong, ACS Mater. Lett., 2021, 3, 379–397.
- 19 Y. Gong, J. Yang, M. Fang and Z. Li, *Cell Rep. Phys. Sci.*, 2022, 3, 100663.
- 20 B. Ding, L. Ma, Z. Huang, X. Ma and H. Tian, *Sci. Adv.*, 2021, 7, eabf9668.
- 21 Y. Zhao, B. Ding, Z. Huang and X. Ma, *Chem. Sci.*, 2022, **13**, 8412–8416.
- 22 S. Jena, A. T. M. Munthasir and P. Thilagar, *J. Mater. Chem. C*, 2022, **10**, 9124–9131.